ILASS-Americas 29th Annual Conference on Liquid Atomization and Spray Systems, Atlanta, GA, May 2017

Experimental characterization of a canonical coaxial gas-liquid atomizer

N Machicoane, and A. Aliseda*
Department of Mechanical Engineering
University of Washington
Seattle, WA 98195-2600 USA

Abstract

Break-up of a liquid jet by a high speed coaxial gas jet is a frequently-used configuration to generate a high quality spray. Despite its extended use in engineering and natural processes, the instabilities that control the liquid droplet size and their spatio-temporal distribution in the spray are not completely understood. Fundamental understanding of the mechanisms that dominate ligament formation and break-up in the liquid, as well as those that determine the differential transport of droplets in the spray can provide quantitative design and analysis tools for spray engineering. Additionally, detailed understanding is necessary to achieve spray control, in which the break up can be actuated to provide certain preferred droplet size distribution, and the dispersion of droplets from the spray axis can be influenced with acoustic or electric forces to achieve a desired spatial distribution.

We present an experimental study of a canonical coaxial gas-liquid atomizer. The liquid injection rate is fixed at a speed of 0.5 m/s (Reynolds number $Re_l = 1000$), while the coaxial gas jet Reynolds number is varied over a wide range $8 \times 10^3 < Re_g < 2 \times 10^6$. The resulting droplet sizes distribution is measured using PDPA in the mid-field region, after the break-up of all fluids ligaments is completed and droplets are spherically-shaped. Data on droplet distribution inside the spray is compared with high-resolution particle-laden DNS from our collaborators at U. Florida. The break-up process and the spray development are also characterized in the close-field region using high-speed imaging. These data sets are complemented with X-ray measurements and liquid-gas interface dynamics capturing numerical simulations of the spray shape and void fraction, presented by our collaborators at Iowa State University and Cornell University. This work is part of a large-scale project funded by an ONR MURI to provide feedback control of sprays.

*Corresponding Author: aaliseda@uw.edu

Atomizer Design Characterization

A two fluid coaxial atomizer has been designed to study atomization physics in a canonical setting. The design focuses on obtaining well-characterized and reproducible laminar liquid and turbulent gas streams. The liquid is introduced via a straight circular duct 100 mm in length and 2 mm in diameter. Fully developed Poiseuille flow is thus the exit condition of the liquid into the atomization process. The gas is injected perpendicular to the axis of the injector through eight inlets (four 1/2" inlets for the no-swirl gas feed, and four 3/8" inlets for the swirl gas feed). It then develops along a 90 mm nozzle whose inner (the outer wall of the liquid duct) and outer surfaces are shaped with cubic splines revolved around the axis of the injector [1]. The drawing of the atomizer is shown in figure 1 and the detailed CAD design will be made available on an open-source repository for the community.

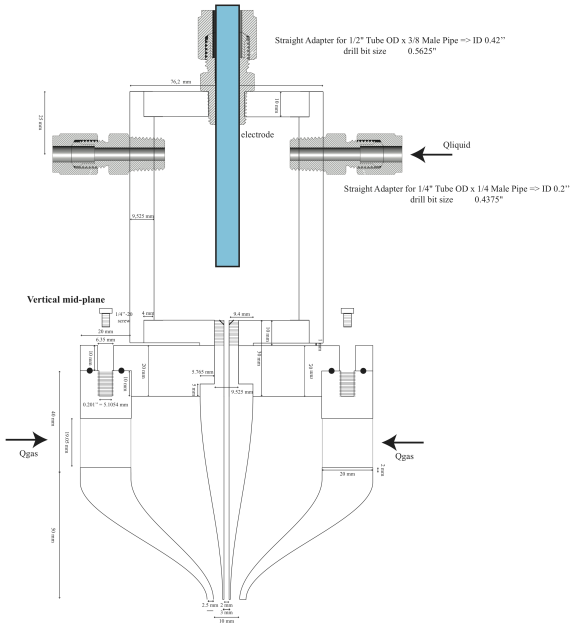

Figure 1. Atomizer Blueprints

Atomization Visualizations

This paper focuses on flow visualization that map the different modes of atomization accessible for study in this coaxial two-fluid atomizer. Specifically, the no-swirl characterization, in a range of Gas Reynolds numbers from $10^4 - 2\ 10^5$ has been explored, keeping the liquid Reynolds number constant at 10^3 to maintain laminar conditions inside the liquid injection duct prior to the nozzle. The Weber number ($We = \rho_g U_g^2 d_l/\sigma$) range explored, based on the gas exit velocity and liquid jet diameter is $10 - 10^4$[2]. Gas flow fields both at the nozzle exit and at different distances downstream throughout the jet development process, as well as droplet size and velocity distributions will be made available for the community for comparison of different experimental techniques applied to spray characterization and for validation of different computational tools for simulation of the liquid jet destabilization and break processes, as well as the droplet transport process within the spray.

Shadowgraphy high speed movies, of which extracted images are shown in figure 3, allow for a qualitative mapping of the different instabilities and atomization modes[3]. At low gas Reynolds, $Re_g \approx 10^4$, and Momentum Ratio values, $M = \rho_g U_g^2/\rho_l U_l^2 \approx 6$, a sinusoidal instability exposes the liquid jet to the high speed gas and results in multibag break up. At intermediate gas Reynolds numbers ($Re_g \approx 5\ 10^4$, $M \approx 30$), the liquid jet accelerates, narrowing sharply within the potential cone of the gas, and suffers from a symmetric varicose instability that exposes the liquid to the high speed gas, with further instability, formation of ligaments and break up[4]. For the highest gas Reynolds numbers ($Re_g > 10^5$, $M > 10^2$), the liquid-gas interface is subject to the classical Kelvin-Helmhotz instability (clearly visible in the intact liquid jet at $Re_g = 97000$ in the lower, left panel of figure 3) the ligaments formed by this instability quickly accelerate and break into individual droplets[5].

Quantitative Analysis from High-Speed Flow Visualizations

In an effort to characterize the integral features of the spray, and to compare against our MURI Spray Control collaborators radiographic measurements [6] and computational simulations [7], we perform quantitative analysis on the whole image sequences (10000 images collected at 11000 fps). The intensity of light transmitted throughout the spray in the back-illuminated high speed movies is qualitatively representative of the volume fraction of liquid in the spray (taking into account that dispersion is a strong function of droplet size)[8]. The statistical description of the resulting synthetic long-exposure images is shown, as contours of average and standard deviation of light intensity, in figures 4 and 5. In these images, there is a clear inflection point between the initial (slow) development of the spray, and the (faster) spreading as the liquid interacts with the bulk of the turbulent gas stream. At higher gas Reynolds numbers, the acceleration of the liquid by the gas stream produces an actual narrowing of

the spray at that critical downstream distance, prior to the faster spray spread characteristic of the mid-field, self-similar jet development.

From the quantitative information in the synthetic long-exposure images shown in figures 4 and 5, evaluated for all Reynolds numbers studied, we determine (within a certain thresholding criteria) the intact length and the spreading angle of the spray. The intact length was defined as the point of the minimum in the mean intensity's second derivative along the longitudinal direction. The spreading angle was defined based on the maximum of the light standard deviation along the radial direction (across the spray). Intensities were in the range [0 2500] for the average and [0 1000] for the standard deviation.

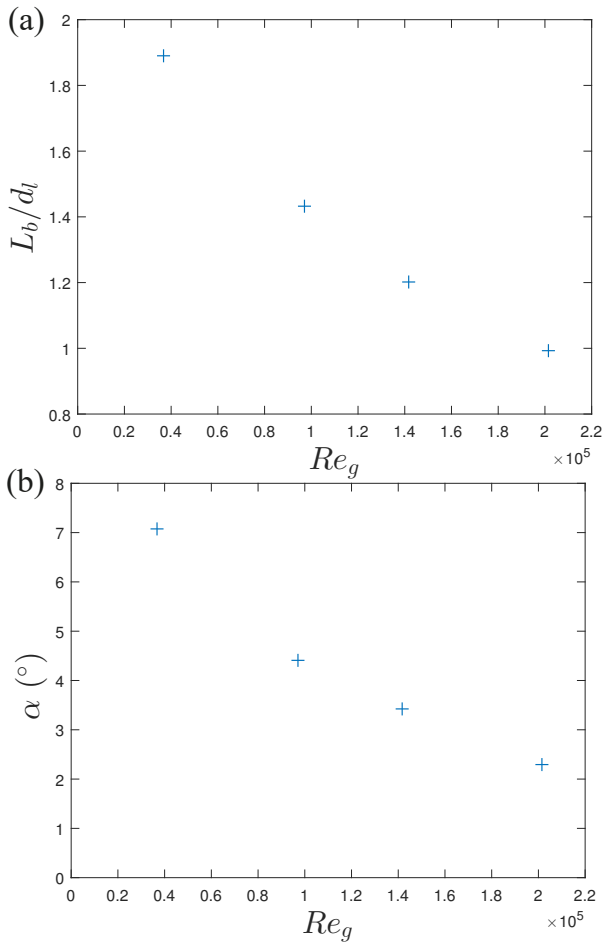

Figure 3. Intact Length (a) and Spreading Angle (b) for the near-field spray development at a range of turbulent gas Reynolds numbers ($Re_g = 10^4 - 2\ 10^5$) and constant liquid Reynolds number ($Re_l = 10^3$), such that the mass ratio, $m = \rho_l U_l / \rho_g U_g$, is small and the momentum ratio, M, is large.

As expected the intact length decreases with increasing gas Reynolds number in the atomizer. This trend is approximately linear between $Re_g = 10^4 - 10^5, M = 6 - 200$ and starts to saturate as the gas Reynolds number increases above 10^5 or the momentum ratio increases beyond 200. Given the uncertainty on the intact length measured for the highest gas Reynolds, caused by the difficulty in differentiating between the lack of light transmission of the intact liquid jet and that of the dense small droplets after break up moving at speeds high enough to blur the image even at the lowest exposure times allowable ($t_{exp} = 285\ 10^{-9}\ s$), comparison with the X-ray radiographic images presented in [6] for all Reynolds numbers studied, at consistent thresholds, provides additional assurance of the robustness of this measurements.

The initial liquid spreading angle also decreases with increasing gas Reynolds numbers. While it is clear that the spreading angle changes in the mid field, as the gas jet develops into a self-similar state, the acceleration of the liquid with increasing gas exit velocity produces a focusing of the spray at a distance downstream $x \approx 10\ D_l$ that, associated with an inflection point in the spreading, strongly influences the transition from the near to the mid field.

Acknowledgements

This work was sponsored by the Office of Naval Research (ONR), as part of the Multidisciplinary University Research Initiatives (MURI) Program, under grant number N00014-16-1-2617. The views and conclusions contained herein are those of the authors only and should not be interpreted as representing those of ONR, the U.S. Navy or the U.S. Government.

References

[1] A. Hussain & V. Ramjee. *Journal of Fluids Engineering*, 3:58–68, 1976.

[2] C.M. Varga, E. J. Hopfinger, and J.C. Lasheras. *J. Fluid Mech.*, 497:405–434, 2003.

[3] P. Marmottant and E. Villermaux. *J. Fluid Mech.*, 498:73–111, 2004.

[4] J. C. Lasheras and E.J. Hopfinger. *Ann. Rev. Fluid Mech.*, 32:275–308, 2000.

[5] A. Aliseda, E. J. Hopfinger, J. C. Lasheras, D. M. Kremer, A. Berchielli, and E. K. Connolly. *Int. J. Multiphase Flow*, 34(2):161–175, 2008.

[6] T.J. Heindel, D. Li, T.B. Morgan, J.K. Bothell, A. Aliseda, N. Machicoane, and A. Kastengren. *Conference on Liquid Atomization and*

Spray Systems, ILASS-Americas, Atlanta, USA, May 2017.

[7] R. Chiodi, L.X. Vu, and O. Desjardins. *Conference on Liquid Atomization and Spray Systems, ILASS-Americas*, Atlanta, USA, May 2017.

[8] Cameron Tropea. *Annual Review of Fluid Mechanics*, 43(1):399–426, 2011.

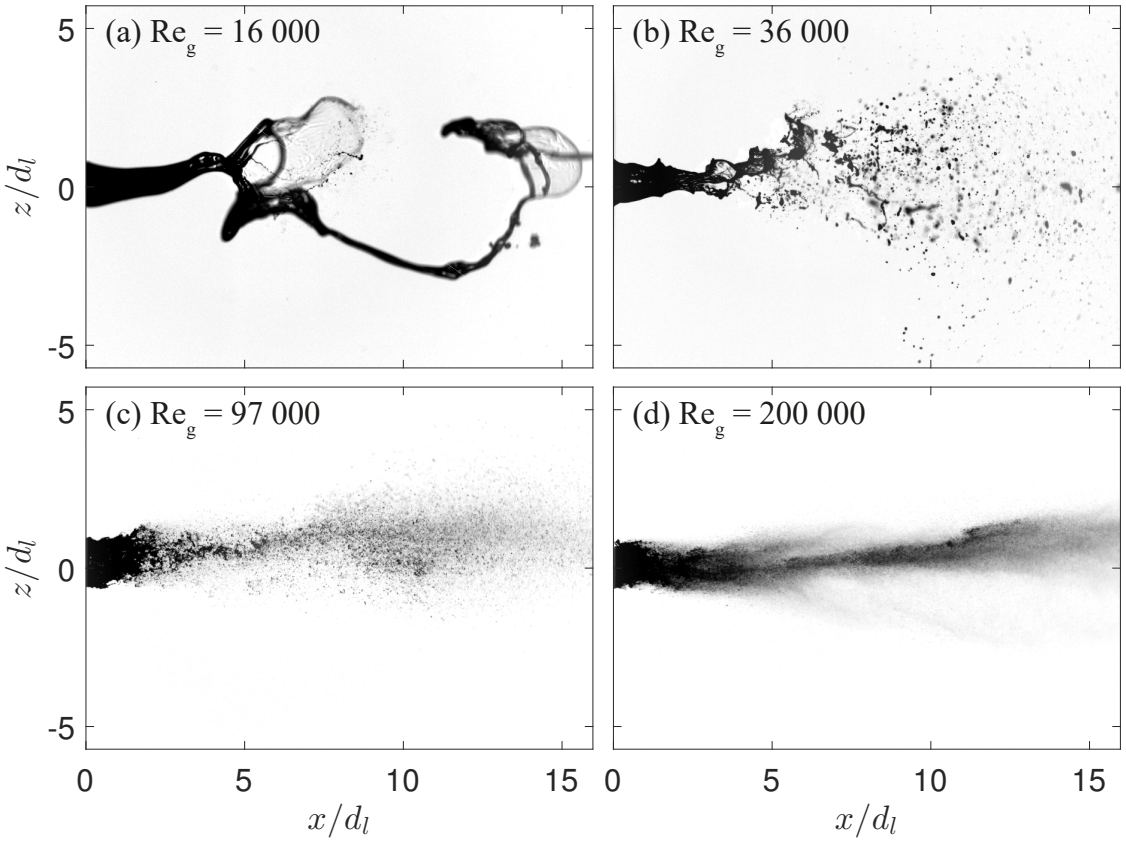

Figure 2. Instantaneous images extracted from high-speed flow visualizations of light scattered by the liquid jet and spray, over a wide range of Gas Reynolds numbers

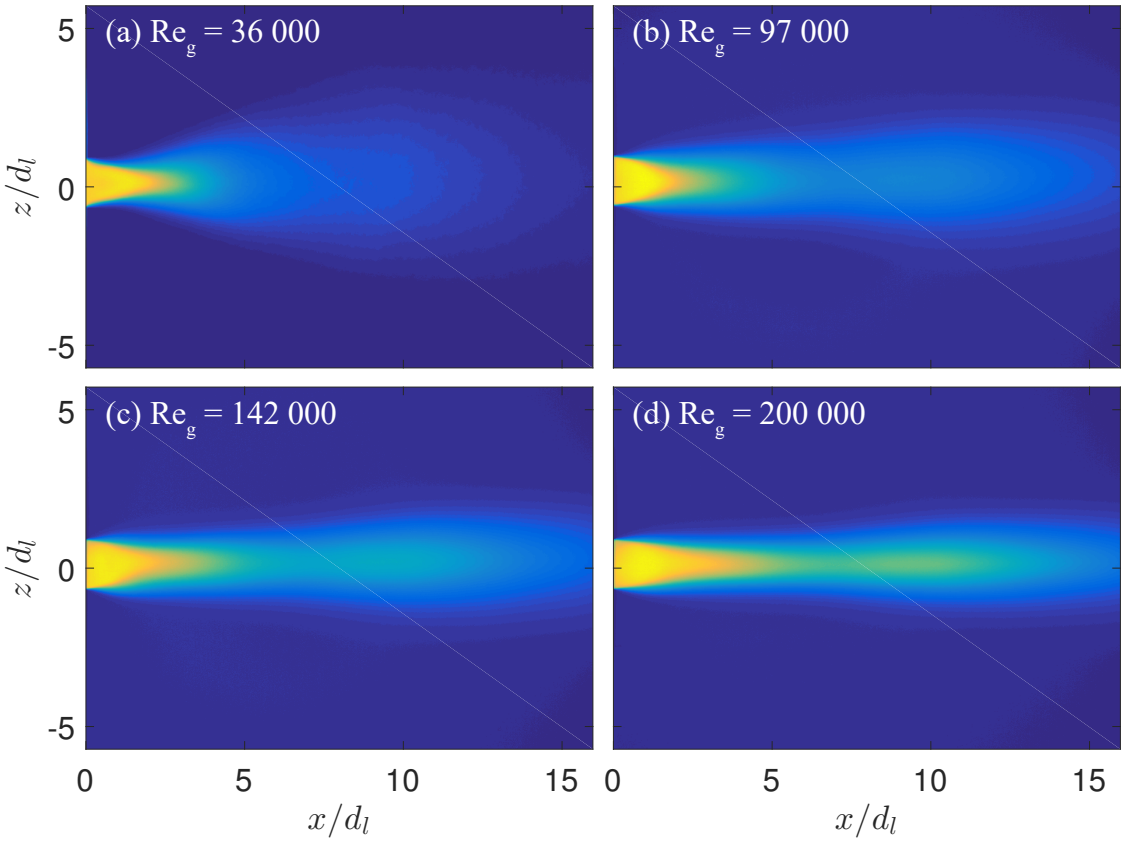

Figure 4. Average light intensity transmitted through the spray. Data used for quantitative analysis of the near-field, including the intact length and spreading angle.

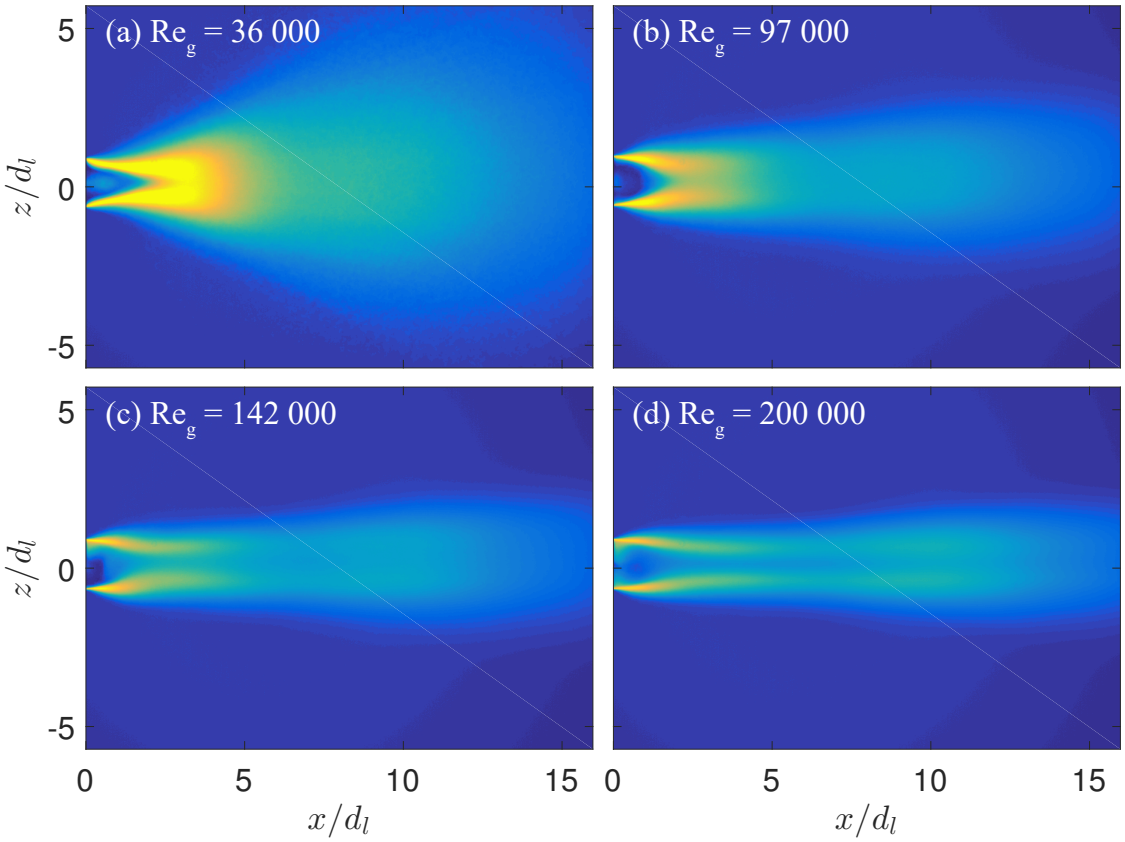

Figure 5. Standard Deviation of light intensity transmitted through the spray. Data used for quantitative analysis of the near-field, including the intact length and spreading angle.